Biophysical Chemistry 160 (2012) 69–74

Contents lists available at SciVerse ScienceDirect

Biophysical Chemistry

journal homepage: http://www.elsevier.com/locate/biophyschem

Short Communication

Mercury inhibits the L170C mutant of aquaporin Z by making waters clog the water channel

Yubo Zhang, Yubao Cui, L.Y. Chen *

Department of Physics, University of Texas at San Antonio, One UTSA Circle, San Antonio, TX 78249, USA

HIGHLIGHTS

- Mercury bonded to residue Cys 170 does not cause consequential changes to the AQPZ-L170C mutant.
- Bonding one mercury to Cys 170 reduces osmotic permeability to half of the mercury-free system.
- It is the electrostatic field of the mercury that makes water molecules clog the water channel of L170C.

GRAPHICAL ABSTRACT

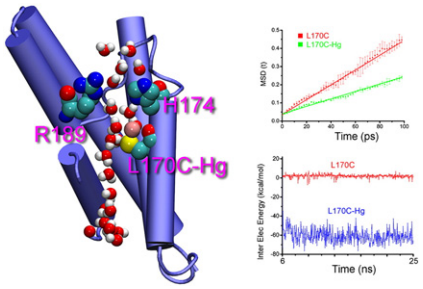

ARTICLE INFO

Article history:
Received 7 June 2011
Received in revised form 14 July 2011
Accepted 25 July 2011
Available online 3 August 2011

Keywords:
Aquaporin inhibition
Osmotic permeation
Molecular dynamics

ABSTRACT

We conduct *in silico* experiments of the L170C mutant of the *Escherichia coli* aquaporin Z (AQPZ) with and without mercury bonded to residue Cys 170. We find that bonding mercury to Cys 170 does not induce consequential structural changes to the protein. We further find that mercury does not stick in the middle of the water channel to simply occlude water permeation, but resides on the wall of the water pore. However, we observe that the water permeation coefficient of L170C-Hg^+ (with one mercury ion bonded to Cys 170) is approximately half of that of the mercury-free L170C. We examine the interactions between the mercury ion and the waters in its vicinity and find that five to six waters are strongly attracted by the mercury ion, occluding the space of the water channel. Therefore we conclude that mercury, at low concentration, inhibits AQPZ-L170C mutant by making water molecules clog the water channel.

Aquaporins (AQPs) are integral membrane channel proteins that mediate the bi-directional flux of water and selected small molecules across the cell membrane [1]. Mercurial compounds were found to inhibit water transport [2] and were used for various *in vitro* analyses of aquaporins [3–10]. It is known that mercury inhibits most AQPs by interacting with the accessible cysteine residues [7]. The current literature provides two mechanisms of inhibition of AQPs by mercury: the first is simple occlusion of the water pore by the mercury atoms/ions found in the vicinity of the cysteine residues lining the water channel wall; the second is conformational change (collapse of the water pore) at the selectivity filter (SF) (namely, the aromatic/arginine (ar/R) constriction) region induced by mercury bonded to a cysteine residue nearby. The simple occlusion mechanism was elucidated from the X-ray crystallographic studies [10] of aquaporin Z from *Escherichia coli* (AQPZ) [11–14] and its mutants. The second mechanism was proposed in an *in silico* study on the basis of molecular dynamics (MD) simulations of the bovine aquaporin AQP1 [15]. In this paper, we present an *in silico* study of the L170C mutant of AQPZ and demonstrate a new mechanism of mercury inhibition: The mercury ion Hg^+ covalently bonded to the cysteine residue (Cys 170)

* Corresponding author.
E-mail address: Liao.Chen@utsa.edu (L.Y. Chen).

0301-4622/$ – see front matter © 2011 Elsevier B.V. All rights reserved.
doi:10.1016/j.bpc.2011.07.006

causes water molecules to clog the water channel. This new mechanism explains L170C's high sensitivity to mercury observed in the *in vitro* functional experiments of Ref. [10].

MD simulations complement *in vitro* experimental studies by providing valuable dynamics information and connecting the dots from the static information in the X-ray structure to the functional experiments such as water transport assays. In the current literature, there are many *in silico* studies of AQPs [15–57], but few on the mercury inhibition of water transport [15]. In order to reveal the mechanism of mercury inhibition of L170C, we present *in silico* studies of the L170C mutant of AQPZ in absence of and in presence of mercurials in the systems. We utilize the widely used MD engine NAMD [58] to perform *in silico* experiments. We use the well tested CHARMM27 force fields [59] to model the intra- and inter-molecular interactions of our all-atom model systems of the cell membrane containing water channel proteins. The first system of our study, illustrated in Fig. 1, consists of an AQPZ-L170C (PDB code: 2O9F) tetramer embedded in a 109Å×109Å patch of POPE lipid bi-layer solvated with TIP3 waters and ionized with NaCl to neutrality and physiological ion concentration. Note that residue His 174 is set to the protonated state and carries a positive charge. The second system of our study is derived from the first system by mutating residue Cys 170 into residue Cys-Hg^+ (the mercury ion Hg^+ takes the place of the γ hydrogen of cysteine) and deprotonating residue His 174 from the positively charged form into the neutral form. Correspondingly, no additional ions are needed to neutralize the second system. We know that the protonation state of a histidine residue is determined by its environment at a neutral pH level of the solution. Therefore, based on the fact that His 174 is in the proximity of Cys 170, we choose His 174 to be deprotonated when Hg^+ is covalently bonded to the S atom of Cys 170. The parameters for the Cys-Hg^+ residue are taken from Ref. [15] that contains an MD study of mercury inhibition of bovine AQP1. Note that the fine features of water–Hg^{2+} interactions have been studied in Refs. [60–62]. Our study shows that these fine features are not necessary to explain the mechanism of mercury inhibiting L170C.

After equilibration, we conducted 30 ns of equilibrium MD simulations for each of the two systems from which we examine the structural stability of the protein. The first question we need to answer: Are there consequential structural changes caused by bonding mercury to Cys 170 whose side chain is on the water channel wall? More specifically, does the water pore collapse anywhere along the channel of L170C-Hg^+ in resemblance to what was observed in Ref. [15]?

In Fig. 2, we show how the structures of L170C and L170C-Hg^+ deviate from their crystallographic structures (PDB codes: 2O9F and 2O9G, respectively) when embedded in the lipid bilayer. Fig. 2A and B shows the root mean square deviations (RMSDs) of the alpha carbons as a function of time. In both cases, the RMSDs stabilize around a value less than 2Å, which means that there are no significant overall changes in the solution structures of the protein mutants from their crystallographic form. However, we still need to answer the question about local structural changes because local changes to the side chains of the residues lining up the water channel can be strongly consequential. Fig. 2C and D demonstrates the water pore radii along the water channel at different times in comparison to the crystallographic structure. We find that nowhere along the water channel does the water pore collapse in either the L170C or the L170C-Hg^+ system. We also find that the mercury ion bonded to Cys 170 does not stick far enough out of the channel wall to occlude the pore space, instead, it remains nearly on the channel wall. The pore radius of L170C-Hg^+ water channel is greater than that of the crystallographic structure (PDB code: 2O9G) that has multiple mercury atoms located in the

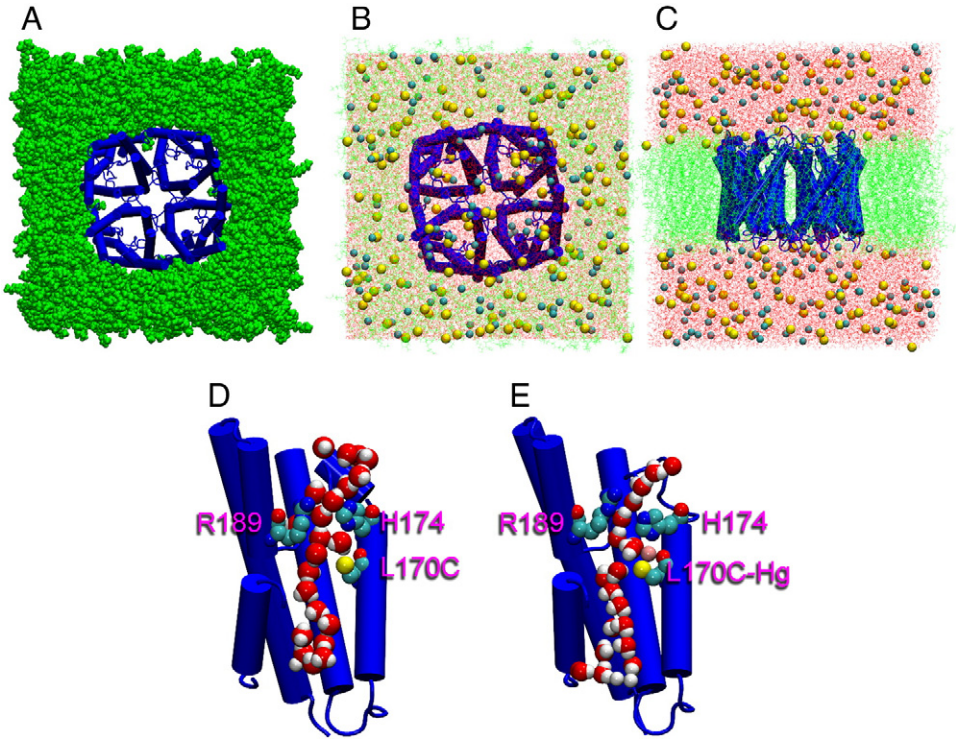

Fig. 1. The all-atom model system consisting of an L170C homotetramer embedded in a patch of POPE bi-layer solvated in a 109Å×109Å×117Å box of waters neutralized and ionized with NaCl to a concentration of 0.15 M. (A) shows only the L170C tetramer (blue) and the patch of lipid bi-layer (cyan). (B) shows the top view and (C), the side view of the system. In (B) and (C), waters are the red dots. Sodium and chlorine ions are shown as yellow and blue spheres respectively. (D) shows one protomer of the L170C mutant of AQPZ along with waters in its pore. (E) shows one protomer of the L170C-Hg mutant of AQPZ along with waters in its pore. In both (D) and (E), residues His 174, Arg 189, Cys 170, and Cys-Hg 170 are shown in VDW representation. Also in VDW are the waters. The graphics were rendered with VMD [64]. The MD simulations were implemented as the Langevin dynamics under constant pressure of 1 bar with periodic boundary conditions. The particle mesh Ewald was employed for long range electrostatic forces. The cutoff distance was set to 12Å with a switching distance of 10Å. The time step was chosen as 2 fs and the damping constant 5/ps.

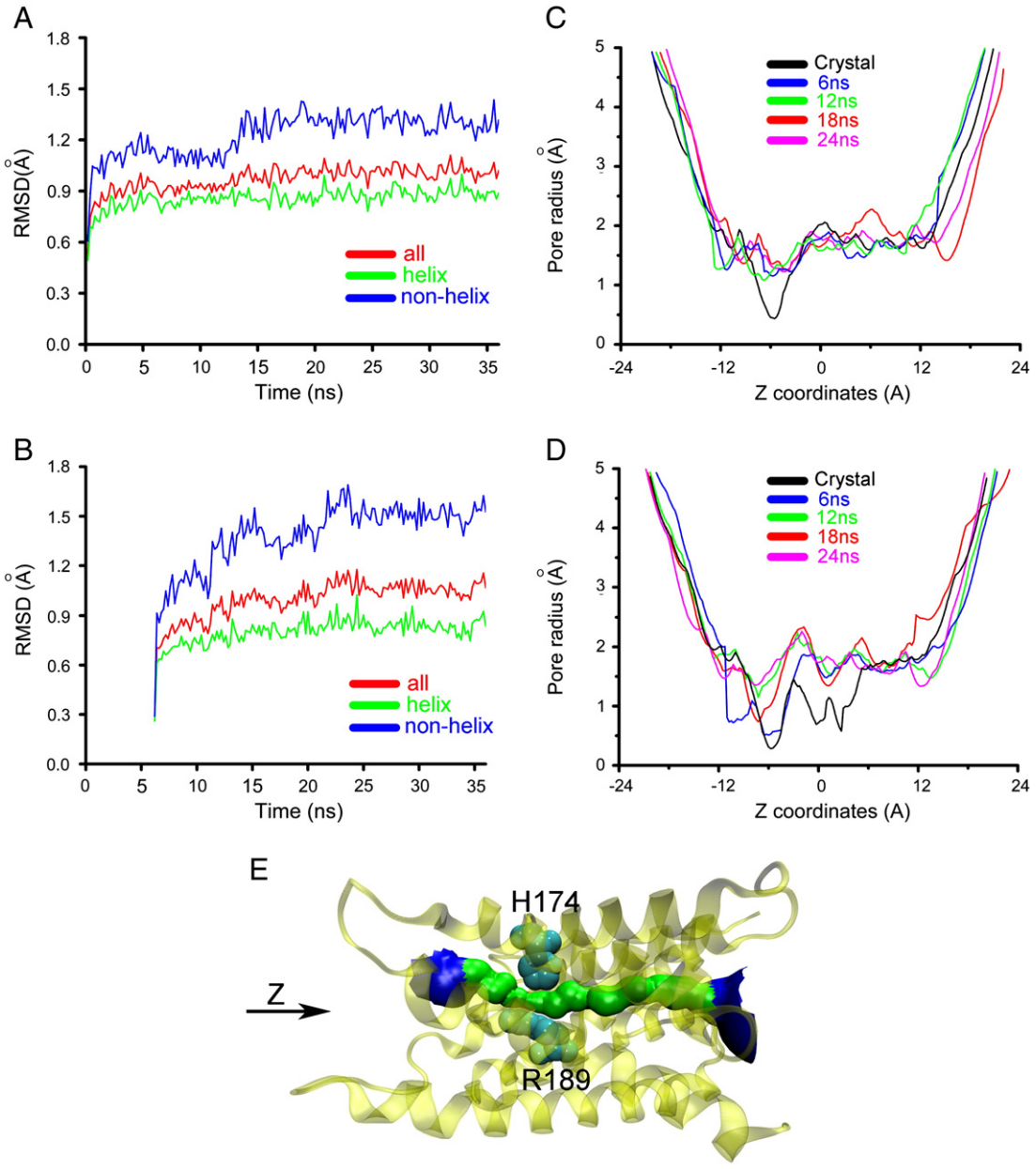

Fig. 2. RMSDs of L170C (A) and L170C-Hg^+ (B) from the crystallographic structure of L170C (PDB code: 2O9F) as a function of time. The initial structure of L170C-Hg^+ is derived from that of L170C after 6 ns of equilibration by mutating Cys 170 and deprotonating His 174. The pore radii along the channel axis (z-axis) at t = 0, 6, 12, 18, and 24 ns for L170C (C) and L170C-Hg^+ (D). The t = 0 snap shots are the crystal structures of L170C (PDB code: 2O9F) and of L107C-Hg (PDB code: 2O9G). (E) illustrates a representative water pore of a protomer. Rendered with VMD [64] and HOLE2 plug-in [65].

middle of the pore. At this point, we can conclude that mercury does not inhibit L170C by structural changes.

Now the next question: Does bonding mercury to Cys 170 actually inhibit water transport through the water channel? This question can be answered directly by the measurements of osmotic permeability from the *in silico* experiments of the L170C and the L170C-Hg^+ systems. Using the theoretical formulation of Ref. [63], we computed the mean square displacements (MSD) of the water molecules in the water pore. The results are shown in Fig. 3(A). From the slope of the MSD *vs* time curves, we can compute the osmotic permeability [63]: the slope is equal to $2D_n$ (D_n being the collective diffusion constant of the waters in the pore) and the osmotic permeability $p_f = v_W D_n$ where v_W is the average volume occupied by one water molecule. For L170C, we have $p_f = 4.4 \pm 0.3 \times 10^{-14}$ cm^3/s, which is identical to what was obtained in Ref. [32] for the wild-type AQPZ in POPE lipid bi-layer. For L170C-Hg+, we have $p_f = 2.0 \pm 0.2 \times 10^{-14}$ cm^3/s. Clearly, the osmotic permeability of L170C-Hg^+ is only half of that of L170C. This corresponds to the half maximal inhibitory concentration, IC_{50}, along the dose–response curve for L170C and explains the high sensitivity of L170C to $HgCl_2$ observed in the water transport assays of Ref. [10]. Even though bonding single mercury to Cys 170 does not cause much steric hindrance in the water pore, it does significantly reduce the osmotic permeability of the channel.

In order to understand how mercury bonding to Cys 170 reduces water permeability without inducing steric hindrance in the water pore, we have computed the potential of mean force (PMF) on the basis of water density along the water channel [16]. The results are shown in Fig. 3(B). The presence of the mercury ion bonded to Cys 170 causes a significant lowering of the PMF around $z = -2$Å where Cys 170 resides, forming a new free-energy well on the PMF profile of L170C-Hg^+. Accordingly, water density in the region becomes higher due to the strong electrostatic attraction between the mercury ion and

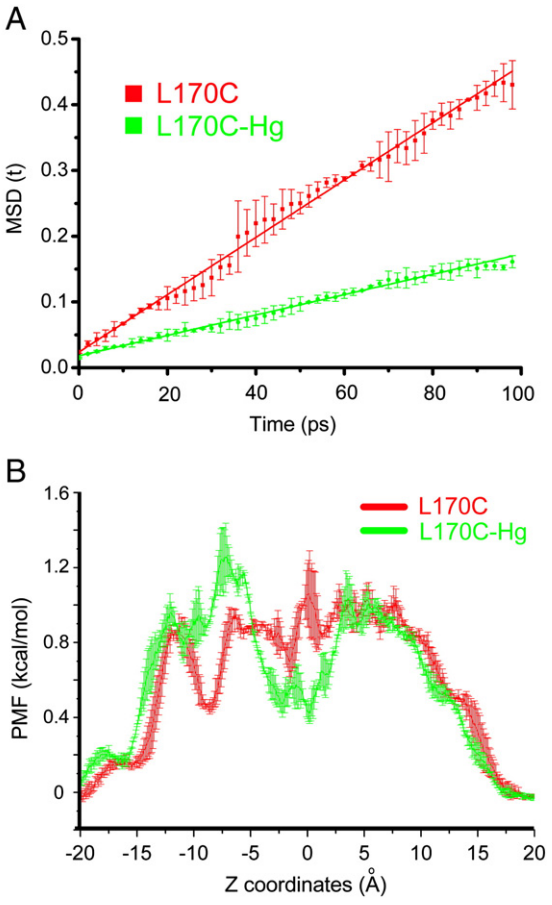

Fig. 3. (A) Mean square displacements (in Å) of waters in the water channel as a function of time (in ps). The mean values and the error bars are computed from two sets of simulation paths. The first set contains 100 paths of 100 ps each that are the consecutive 100 ps-segments of the simulation sampling from 16 to 26 ns. The second set consists of the same from the simulation from 26 to 36 ns. The simulation from 0 to 16 ns was to equilibrate the system after embedding the protein to the lipid bi-layer and melting the lipid tails. (B) Potential of mean force computed from the water density profile along the water channel. The mean values and the error bars are computed from two sets of data that were obtained from simulations of 16 to 26 ns and from 26 to 36 ns for each system. The PMF was computed as $\Delta G(z) = -k_B T \ln[n(z)/n_0]$ where z is the coordinate along the water channel pointing along the direction from the periplasm to the cytoplasm, $n(z)$ is number density of waters in a water channel, and $n_0 = n(z = 20\text{Å})$ is the reference density chosen to be at $z = 20$Å.

the waters in its vicinity as shown in Fig. 4. This altered PMF profile divides the stochastic process of a water molecule permeating the water pore into two processes. When a water molecule enters the water pore from the vestibule on the extracellular side of the membrane, it overcomes the free-energy barrier in the ar/R region (around $z = -7$Å). It then dwells in the free-energy well in the vicinity of the Cys-Hg^+ 170 residue. From there, it overcomes a second free-energy barrier near the NPA motifs before traversing onto the cytoplasm side of the membrane. Thus it is the dwelling waters that clog up the water channel and hinder the permeation flow of water. It is also noted that the Na^+ and Cl^- ions do not enter into the water channels, which is consistent with the known fact that aquaporin water channels do not allow permeation of ions.

Based on the *in silico* experiments of the AQPZ-L170C mutant with or without a mercury ion bonded its Cys 170 residue, we find that mercury does not inhibit L170C by inducing significant structural changes in the protein or by directly occluding the water channel but, instead, it does so by making water molecules clog the water channel. Our model system of L170C-Hg^+ does not involve more than one mercury atoms/ions in a given water pore. It is relevant to *in vitro* experiments at low concentrations of mercury. At low mercury concentrations, the probability for multiple mercury atoms/ions to exist in any given water pore should be small. The most probable case is that one mercury ion is covalently bonded to the Cys 170 residue. Finally, in this *in silico* study, we use a planar POPE bi-layer to model the cell membrane, which is not exactly identical to the membrane of the proteoliposomes used in the *in vitro* experiments of Ref. [10]. It is true that the liposome curvature is neglected in our planar lipid bi-layer. However, considering the fact that L170C structure does not deviate significantly in presence or in absence of mercury, no significant effects are expected from the membrane curvature. Also, the phospholipid headgroups of the proteoliposomes may be charged but the POPE headgroups are neutral (though highly polar). This difference is not expected to cause any problems because both sides of the membrane are fully solvated with sufficient amount of water having appropriate concentration of Na^+ and Cl^- ions.

Acknowledgments

The authors acknowledge support from an NIH SC3 grant (GM084834), the UTSA Computational Biology Initiative, and the Texas Advanced Computing Center.

References

[1] M. Borgnia, et al., Cellular and molecular biology of the aquaporin water channels, Annu. Rev. Biochem. 68 (1999) 425–458.
[2] R.I. Macey, Transport of water and urea in red blood cells, Am. J. Physiol. Cell Physiol. 15 (2) (1984) 9.
[3] M.L. Zeidel, et al., Reconstitution of functional water channels in liposomes containing purified red-cell Chip28 protein, Biochemistry 31 (33) (1992) 7436–7440.
[4] G.M. Preston, et al., Appearance of water channels in Xenopus oocytes expressing red-cell Chip28 protein, Science 256 (5055) (1992) 385–387.
[5] K. Fushimi, et al., Cloning and expression of apical membrane water channel of rat-kidney collecting tubule, Nature 361 (6412) (1993) 549–552.
[6] H. Javot, C. Maurel, The role of aquaporins in root water uptake, Ann. Bot. 90 (3) (2002) 301–313.
[7] G.M. Preston, et al., The mercury-sensitive residue at cysteine-189 in the Chip28 water channel, J. Biol. Chem. 268 (1) (1993) 17–20.
[8] K.Y. Kuang, et al., Mercurial sensitivity of aquaporin 1 endofacial loop B residues, Protein Sci. 10 (8) (2001) 1627–1634.
[9] R. Zhang, et al., A point mutation at cysteine 189 blocks the water permeability of rat kidney water channel CHIP28k, Biochemistry 32 (12) (1993) 2938–2941.
[10] D.F. Savage, R.M. Stroud, Structural basis of aquaporin inhibition by mercury, J. Mol. Biol. 368 (3) (2007) 607–617.
[11] M.J. Borgnia, et al., Functional reconstitution and characterization of AqpZ, the *E-coli* water channel protein, J. Mol. Biol. 291 (5) (1999) 1169–1179.
[12] M.J. Borgnia, P. Agre, Reconstitution and functional comparison of purified GlpF and AqpZ, the glycerol and water channels from *Escherichia coli*, Proc. Natl Acad. Sci. 98 (5) (2001) 2888–2893.
[13] G. Calamita, et al., Molecular-cloning and characterization of Aqpz, a water channel from *Escherichia-coli*, J. Biol. Chem. 270 (49) (1995) 29063–29066.
[14] D.F. Savage, et al., Architecture and selectivity in aquaporins: 2.5Å x-ray structure of aquaporin Z, PLoS Biol. 1 (3) (2003) e72.
[15] Y. Hirano, et al., Molecular mechanisms of how mercury inhibits water permeation through aquaporin-1: understanding by molecular dynamics simulation, Biophys. J. 98 (8) (2010) 1512–1519.
[16] B.L. de Groot, H. Grubmuller, Water permeation across biological membranes: mechanism and dynamics of aquaporin-1 and GlpF, Science 294 (5550) (2001) 2353–2357.
[17] Y. Kong, J. Ma, Dynamic mechanisms of the membrane water channel aquaporin-1 (AQP1), Proc. Natl. Acad. Sci. U. S. A. 98 (25) (2001) 14345–14349.
[18] M.S. Sansom, et al., Water in ion channels and pores—simulation studies, Novartis Found. Symp. 245 (2002) 66–78 discussion 79–83, 165–8.
[19] E. Tajkhorshid, et al., Control of the selectivity of the aquaporin water channel family by global orientational tuning, Science 296 (5567) (2002) 525–530.
[20] B.L. de Groot, et al., The mechanism of proton exclusion in the aquaporin-1 water channel, J. Mol. Biol. 333 (2) (2003) 279–293.
[21] M.O. Jensen, E. Tajkhorshid, K. Schulten, Electrostatic tuning of permeation and selectivity in aquaporin water channels, Biophys. J. 85 (5) (2003) 2884–2899.
[22] S. Biswas, Functional properties of soybean nodulin 26 from a comparative three-dimensional model, FEBS Lett. 558 (1–3) (2004) 39–44.
[23] R.J. Law, M.S. Sansom, Homology modelling and molecular dynamics simulations: comparative studies of human aquaporin-1, Eur. Biophys. J. 33 (6) (2004) 477–489.
[24] P. Vidossich, M. Cascella, P. Carloni, Dynamics and energetics of water permeation through the aquaporin channel, Proteins 55 (4) (2004) 924–931.
[25] F. Zhu, E. Tajkhorshid, K. Schulten, Theory and simulation of water permeation in aquaporin-1, Biophys. J. 86 (1 Pt 1) (2004) 50–57.

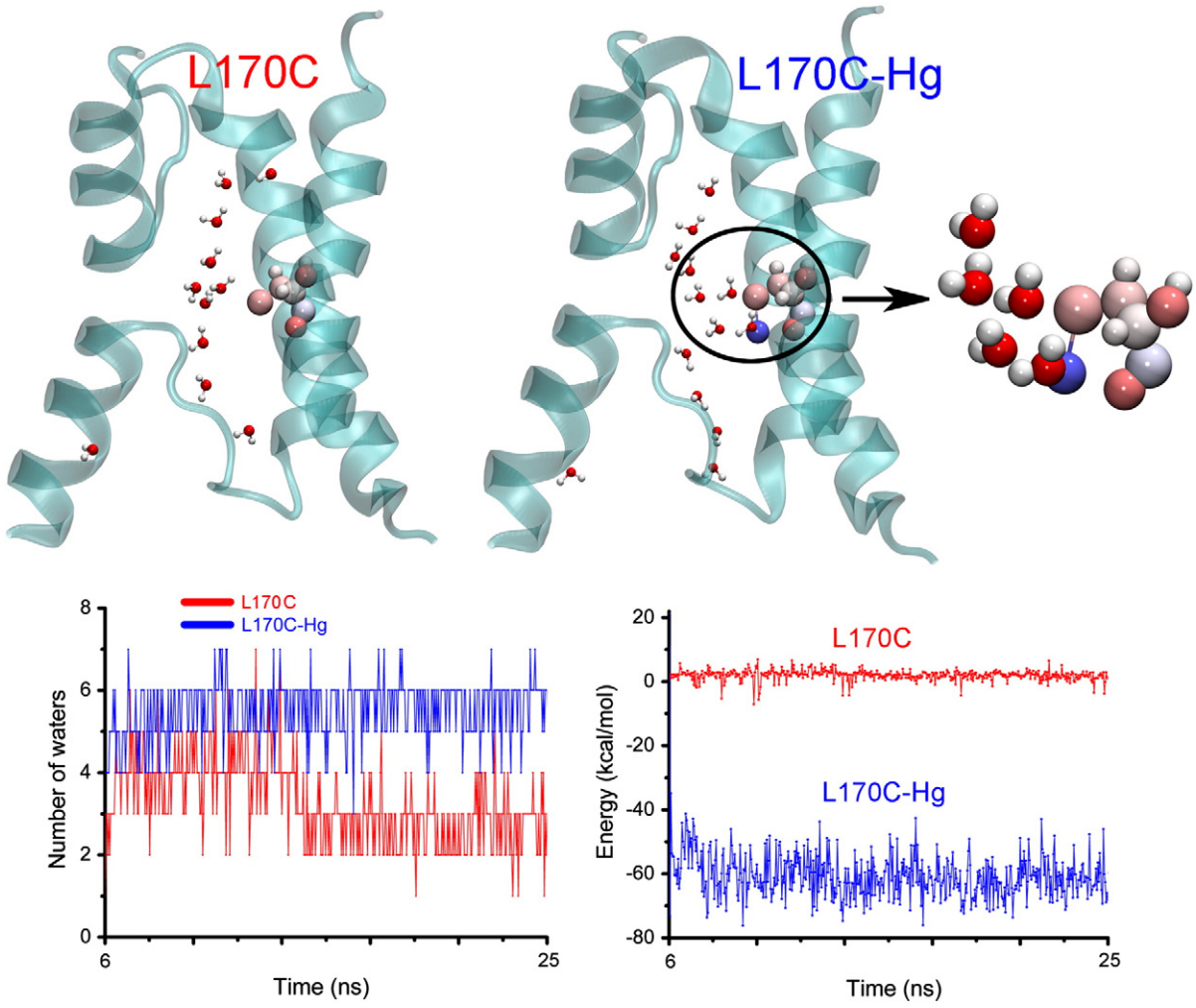

Fig. 4. Waters near residue 170 (Cys or Cys-Hg^{+}) and their electrostatic energy with residue 170. Shown in the top are representative snapshots of a protomer with waters in its pore. Cys 170 and Cys-Hg^{+} 170 are shown in the VDW and the waters in the CPK representation. Shown in the bottom left is the number of waters within 5Å of residue 170. Shown in the bottom right is the electrostatic energy of those waters with residue 170. Rendered with VMD [65].

[26] B.L. de Groot, H. Grubmuller, The dynamics and energetics of water permeation and proton exclusion in aquaporins, Curr. Opin. Struct. Biol. 15 (2) (2005) 176–183.
[27] M. Hashido, M. Ikeguchi, A. Kidera, Comparative simulations of aquaporin family: AQP1, AQPZ, AQP0 and GlpF, FEBS Lett. 579 (25) (2005) 5549–5552.
[28] H. Chen, Y. Wu, G.A. Voth, Origins of proton transport behavior from selectivity domain mutations of the aquaporin-1 channel, Biophys. J. 90 (10) (2006) L73–L75.
[29] F.J. Detmers, et al., Quaternary ammonium compounds as water channel blockers. Specificity, potency, and site of action, J. Biol. Chem. 281 (20) (2006) 14207–14214.
[30] B.G. Han, et al., Water transport in AQP0 aquaporin: molecular dynamics studies, J. Mol. Biol. 360 (2) (2006) 285–296.
[31] J.S. Hub, B.L. de Groot, Does CO2 permeate through aquaporin-1? Biophys. J. 91 (3) (2006) 842–848.
[32] M.O. Jensen, O.G. Mouritsen, Single-channel water permeabilities of *Escherichia coli* aquaporins AqpZ and GlpF, Biophys. J. 90 (7) (2006) 2270–2284.
[33] S. Tornroth-Horsefield, et al., Structural mechanism of plant aquaporin gating, Nature 439 (7077) (2006) 688–694.
[34] H. Chen, et al., Charge delocalization in proton channels, I: the aquaporin channels and proton blockage, Biophys. J. 92 (1) (2007) 46–60.
[35] M. Hashido, A. Kidera, M. Ikeguchi, Water transport in aquaporins: osmotic permeability matrix analysis of molecular dynamics simulations, Biophys. J. 93 (2) (2007) 373–385.
[36] A.B. Mamonov, et al., Water and deuterium oxide permeability through aquaporin 1: MD predictions and experimental verification, J. Gen. Physiol. 130 (1) (2007) 111–116.
[37] Y. Wang, et al., Exploring gas permeability of cellular membranes and membrane channels with molecular dynamics, J. Struct. Biol. 157 (3) (2007) 534–544.
[38] Y. Wang, E. Tajkhorshid, Molecular mechanisms of conduction and selectivity in aquaporin water channels, J. Nutr. 137 (6 Suppl. 1) (2007) 1509S–1515S discussion 1516S–1517S.
[39] M.O. Jensen, et al., Dynamic control of slow water transport by aquaporin 0: implications for hydration and junction stability in the eye lens, Proc Natl Acad Sci U S A 105 (38) (2008) 14430–14435.
[40] Y.J. Ko, J. Huh, W.H. Jo, Ion exclusion mechanism in aquaporin at an atomistic level, Proteins 70 (4) (2008) 1442–1450.
[41] E.M. Muller, et al., Is TEA an inhibitor for human Aquaporin-1? Pflugers Arch. 456 (4) (2008) 663–669.
[42] N. Smolin, et al., Side-chain dynamics are critical for water permeation through aquaporin-1, Biophys. J. 95 (3) (2008) 1089–1098.
[43] R.O. Dror, M.O. Jensen, D.E. Shaw, Elucidating membrane protein function through long-timescale molecular dynamics simulation, Conf Proc IEEE Eng Med Biol Soc, 2009, 2009, pp. 2340–2342.
[44] G. Fischer, et al., Crystal structure of a yeast aquaporin at 1.15 angstrom reveals a novel gating mechanism, PLoS Biol. 7 (6) (2009) e1000130.
[45] J.S. Hub, H. Grubmuller, B.L. de Groot, Dynamics and energetics of permeation through aquaporins. What do we learn from molecular dynamics simulations? Handb. Exp. Pharmacol. 190 (2009) 57–76.
[46] H. Khandelia, M.O. Jensen, O.G. Mouritsen, To gate or not to gate: using molecular dynamics simulations to morph gated plant aquaporins into constitutively open conformations, J. Phys. Chem. B. 113 (15) (2009) 5239–5244.
[47] U. Ludewig, M. Dynowski, Plant aquaporin selectivity: where transport assays, computer simulations and physiology meet, Cell. Mol. Life Sci. 66 (19) (2009) 3161–3175.
[48] C. Aponte-Santamaria, J.S. Hub, B.L. de Groot, Dynamics and energetics of solute permeation through the *Plasmodium falciparum* aquaglyceroporin, Phys. Chem. Chem. Phys. 12 (35) (2010) 10246–10254.
[49] L.Y. Chen, Free-energy landscape of glycerol permeation through aquaglyceroporin GlpF determined from steered molecular dynamics simulations, Biophys. Chem. 151 (3) (2010) 178–180.
[50] L.Y. Chen, D.A. Bastien, H.E. Espejel, Determination of equilibrium free energy from nonequilibrium work measurements, Phys. Chem. Chem. Phys. 12 (25) (2010) 6579–6582.

[51] X. Deupi, et al., Influence of the g-conformation of Ser and Thr on the structure of transmembrane helices, J. Struct. Biol. 169 (1) (2010) 116–123.
[52] J.S. Hub, et al., Voltage-regulated water flux through aquaporin channels in silico, Biophys. J. 99 (12) (2010) L97–L99.
[53] H. Qiu, et al., Dynamic and energetic mechanisms for the distinct permeation rate in AQP1 and AQP0, Biochim. Biophys. Acta 1798 (3) (2010) 318–326.
[54] Y. Wang, E. Tajkhorshid, Nitric oxide conduction by the brain aquaporin AQP4, Proteins 78 (3) (2010) 661–670.
[55] L.Y. Chen, Exploring the free-energy landscapes of biological systems with steered molecular dynamics, Phys. Chem. Chem. Phys. 13 (13) (2011) 6176–6183.
[56] J.A. Garate, N.J. English, J.M. MacElroy, Human aquaporin 4 gating dynamics in dc and ac electric fields: a molecular dynamics study, J. Chem. Phys. 134 (5) (2011) 055110.
[57] H. Li, et al., Enhancement of proton conductance by mutations of the selectivity filter of aquaporin-1, J. Mol. Biol. 407 (4) (2011) 607–620.
[58] J.C. Phillips, et al., Scalable molecular dynamics with NAMD, J. Comput. Chem. 26 (16) (2005) 1781–1802.
[59] A.D. MacKerell, N. Banavali, N. Foloppe, Development and current status of the CHARMM force field for nucleic acids, Biopolymers 56 (4) (2000) 257–265.
[60] V. Migliorati, et al., Effect of the Zn2+ and Hg2+ ions on the structure of liquid water, J. Phys. Chem. A 115 (18) (2011) 4798–4803.
[61] B.M. Rode, C.F. Schwenk, A. Tongraar, Structure and dynamics of hydrated ions—new insights through quantum mechanical simulations, J. Mol. Liq. 110 (1–3) (2004) 105–122.
[62] G. Mancini, et al., Structural and dynamical properties of the Hg2+ aqua ion: a molecular dynamics study, J. Phys. Chem. B 112 (15) (2008) 4694–4702.
[63] F. Zhu, E. Tajkhorshid, K. Schulten, Collective diffusion model for water permeation through microscopic channels, Phys. Rev. Lett. 93 (22) (2004) 224501.
[64] W. Humphrey, A. Dalke, K. Schulten, VMD: visual molecular dynamics, J. Mol. Graph. 14 (1) (1996) 33–38.
[65] O.S. Smart, J.M. Goodfellow, B.A. Wallace, The pore dimensions of gramicidin A, Biophys. J. 65 (6) (1993) 2455–2460.